Dynamic fluid redistribution in hyperosmotic resuscitation of hypovolemic hemorrhage

MICHELLE C. MAZZONI, PER BORGSTRÖM,
KARL-E. ARFORS, AND MARCOS INTAGLIETTA
Department of Applied Mechanics and Engineering Sciences-Bioengineering, University of California, San Diego, La Jolla 92093; and Pharmacia Experimental Medicine, La Jolla, California 92037

MAZZONI, MICHELLE C., PER BORGSTRÖM, KARL-E. ARFORS, AND MARCOS INTAGLIETTA. *Dynamic fluid redistribution in hyperosmotic resuscitation of hypovolemic hemorrhage.* Am. J. Physiol. 255 (Heart Circ. Physiol. 24): H629–H637, 1988.— A mathematical description of blood volume restoration after hemorrhage with resuscitative fluids, particularly hyperosmotic solutions, is presented. It is based on irreversible thermodynamic transport equations and known physiological data. The model shows that after a 20% hemorrhage, the rapid addition of a hypertonic (7.5% NaCl)-hyperoncotic (6% Dextran 70) solution amounting to one-seventh of the shed blood volume reestablishes blood volume within 1 min. Measurements of systemic hematocrit, hemoglobin concentration, and plasma osmolality taken from 13 experiments on anesthetized rabbits verify this prediction. The model shows that immediately after hyperosmotic infusion, water shifts into the plasma first from red blood cells and endothelium and then from the interstitium and tissue cells. The increase in blood volume is transitory; however, it occurs in a fraction of the time compared with isoosmotic fluids at the same infusion rate and is partially sustained by Dextran 70. We theorize that the concurrent hemodilution and endothelial cell shrinkage during hyperosmotic infusion lead to a decreased capillary hydraulic resistance, an effect that is even more significant in capillaries with swollen endothelium. Our results support the significant role of an osmotic mechanism during hyperosmotic resuscitation in quickly restoring blood volume with the added benefit of improved tissue perfusion.

rabbit; hyperosmotic solutions; osmolarity

HYPERTONIC SALINE SOLUTIONS have been shown to successfully restore cardiovascular function when used for the treatment of hypotensive hemorrhage (10, 17, 27, 29). Mean arterial pressure and cardiac output in most cases fully recover after resuscitation, presumably partially because of increased myocardial contractility (30), venoconstriction (14), and precapillary vasoconstriction in muscle and skin (23). The plasma volume is sufficiently reestablished although the infused hyperosmotic fluid volume is only about one-tenth of the shed blood volume. Expansion of the plasma volume is attributed to an osmotic fluid shift into the vascular compartment from intra- and extracellular fluid reservoirs.

In this study, we investigated with experimental and analytical methods the magnitude and time course of the fluid shifts that occur in the body after hemorrhage and subsequent reinfusion of a hypertonic (7.5% NaCl)-hyperoncotic (6% Dextran 70) solution. This mixture was chosen, since it has been shown to be superior to hypertonic saline (7.5% NaCl with no dextran) and other hypertonic solutions in maintaining cardiac output, arterial pressure, and plasma volume (27). The experimental model selected was a 20% hemorrhage in 1 min with prompt hyperosmotic reinfusion carried out on anesthetized rabbits. A mathematical model was developed to analyze the dynamics of fluid redistribution resulting from an osmotic disturbance. It calculates the contribution of each fluid compartment in the body to blood volume restoration.

METHODS

Mathematical analysis. The model is composed of a series of well-mixed fluid compartments. The intracellular fluid is divided into three distinct compartments: red blood cells, vascular endothelium, and tissue cells. The extracellular fluid under normal conditions can move freely between the interstitium and the plasma, but these extracellular spaces are taken as separate compartments, since plasma contains a higher protein concentration, and it is the fluid compartment that receives the hyperosmotic solution. A diagram of the fluid compartment model is shown in Fig. 1. This is a whole body model, but the exchange of water and solutes is a process exclusive to the microcirculation, i.e., the capillaries and postcapillary venules of an organ. The term capillary is used throughout the text to refer to these exchange vessels.

The initial values for the fluid volumes in each compartment are given in Table 1 for a 70-kg person. The plasma volume (PV) and red blood cell volume (RBCV) are dependent on the systemic hematocrit [Hct = RBCV/(PV + RBCV)], which is normally 40–45% of the blood volume. A 20% osmotic dead space (due to solutes and nonsolvent cellular water) is assumed for the red blood cell; multiplying the total RBCV by 80% gives its volume of exchangeable fluid. Hemoglobin concentration in the red blood cell is 32 g/dl. The endothelium fluid volume of 1.5 liter (F. Hammersen, personal communication, 1987) includes the entire vascular tree.

The compartments are separated by membranes that are characterized with a reflection coefficient (σ), hydraulic conductivity (L_p), surface area (S), and solute

permeability-surface area product (PS). Table 2 gives the values of the membrane properties that are taken to be representative of skeletal muscle, since this comprises 65% of the tissue mass available for capillary exchange (11). This tissue mass is assumed to be 60% of the total body weight. It is further assumed that these properties do not change with hemorrhage or hyperosmotic resuscitation, although sustained exposure to elevated osmolarities may increase microvascular permeability in skeletal muscle (2).

References are given for most of the properties in Table 2. The values are extracted directly from the literature; however, a few in particular need to be explained in greater detail. A wide range of permeabilities is reported for albumin and dextrans, presumably due to the use of different measurement techniques. The results of Garlick and Renkin (3), based on the ratio of lymph to plasma concentrations in the dog hindlimb, were employed for the model. Albumin permeability was taken from the experiments with the lowest reported lymph flow rates (passive limb movement was used to enhance lymph flow), and Dextran 70 permeability was computed from their result that the dextran to albumin permeability ratio was about one-third. The surface area of the tissue cells was calculated using the finding that there are on average 3.2–4 capillaries for each muscle cell (21) and that the average diameters of capillary and muscle cell are 5 and 50 μm, respectively.

Values for the hydraulic conductivities of the endothelial membrane and the pores are not available in the literature, however, they can be determined with the use of parallel and series pathway models (7) and known conductivity values. The hydraulic conductivity across the endothelium [luminal (lum) and abluminal (abl) endothelial membranes in series] can be approximated from the conductivity value in brain capillaries. Morphological evidence shows that these capillaries possess no pores (19) and thus their conductivity reflects that of the endothelium. The conductivity of endothelial cells throughout the body is taken to be the same. The hydraulic conductivity of a single endothelial membrane can be calculated from the expression

$$1/L_p^{EC\,br} = 1/L_p^{EC\,lum} + 1/L_p^{EC\,abl} \quad (1)$$

where $L_p^{EC\,br}$ is the conductivity of the brain capillary, and $L_p^{EC\,lum}$ and $L_p^{EC\,abl}$ equals L_p^{EC}, which is the conductivity of a single endothelial membrane. The pore hydraulic conductivity is solved for using $L_p^{EC\,br}$ and the conductivity of the entire capillary (L_p^{cap}). The expression for the hydraulic conductivity of the composite parallel membrane, i.e. the capillary, is

$$L_p^{cap} = \alpha^{EC} L_p^{EC\,br} + \alpha^{pore} L_p^{pore} \quad (2)$$

where L_p^{pore} is the conductivity of the pore, and α^{EC}, α^{pore} denote the fractions of the membrane's area occupied by endothelium and pores, respectively.

All the membranes are permeable to water but have different permeability for other substances. Cellular membranes are semipermeable, allowing only water and no solute to pass through them, i.e., $\sigma = 1$ and $PS = 0$. The capillary wall is a composite membrane that partitions the extracellular compartment and is structurally represented as two identical endothelial membranes in series, which are in parallel with intercellular pores. The pores are taken as the only pathway for solute transport between extracellular compartments with a collective area equal to 0.1% of the capillary surface area (8). The pore can be conceptualized as an open membrane that freely passes sodium chloride (M_r 58.5) but almost completely restricts albumin (M_r 69,000) and dextran (M_r 70,000) with complete exclusion of globulins (M_r 90,000+) and other impermeant macromolecules.

The reflection coefficient of the entire capillary wall (σ^{cap}) is the weighted sum of the reflection coefficients of

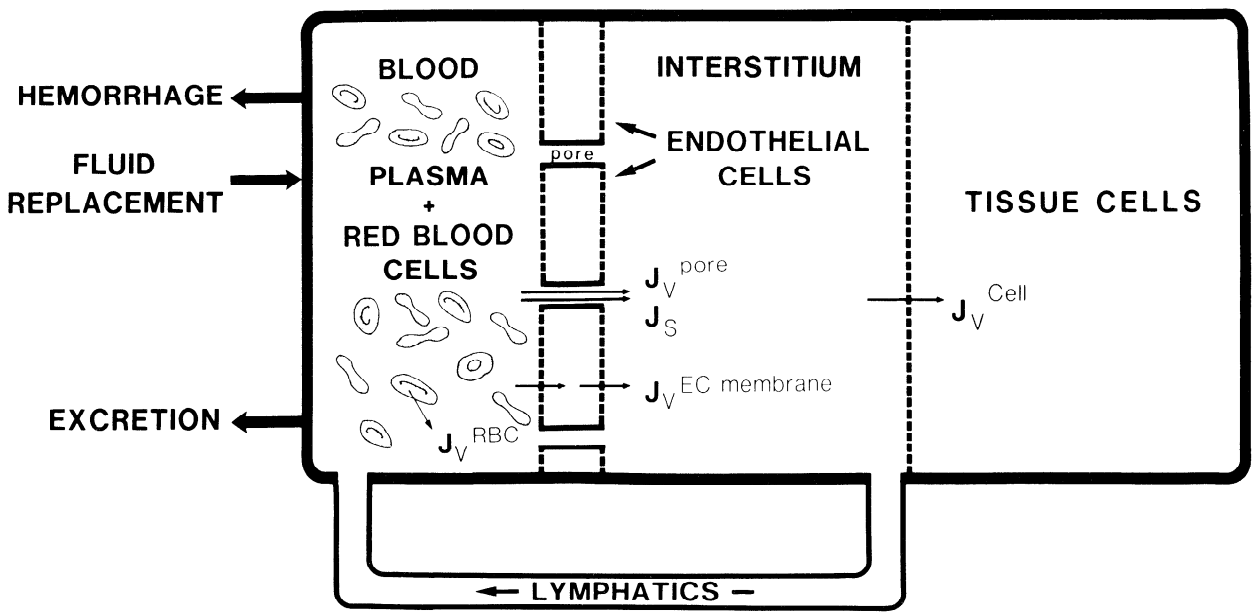

FIG. 1. Diagram of fluid compartments and pathways of fluid exchange in model. Volume (J_v) and solute (J_s) flows across membranes are explained in text.

TABLE 1. *Initial compartmental fluid volume values for a 70-kg person*

Compartmental Fluid Volumes, liters	
Blood	5.0
Plasma	(1 − Hct)·5.0
Red blood cells	0.8·(Hct·5.0)
Endothelium	1.5
Interstitium	10.0
Tissue cells	20.0

Hct, hematocrit.

TABLE 2. *Membrane properties*

σ^{salt}	0	
σ^{alb}	0.9	
σ^{glob}	1	
σ^{dex}	0.8	(5)
$L_p^{EC\ br}$	1.1×10^{-6} ml·min^{-1}·mmHg^{-1}·cm^{-2}	(19)
L_p^{EC}	2.2×10^{-6} ml·min^{-1}·mmHg^{-1}·cm^{-2}	*Eq. 1*
L_p^{cap}	8.1×10^{-6} ml·min^{-1}·mmHg^{-1}·cm^{-2}	(26)
L_p^{pore}	3.5×10^{-6} ml·min^{-1}·mmHg^{-1}·cm^{-2}	*Eq. 2*
L_p^{RBC}	7.2×10^{-7} ml·min^{-1}·mmHg^{-1}·cm^{-2}	(24)
$L_p^{t\ cell}$	1.3×10^{-6} ml·min^{-1}·mmHg^{-1}·cm^{-2}	(6)
S^{cap}	70 cm^2/g tissue	(11)
S^{EC}	$0.999 \cdot S^{cap}$	
S^{pore}	$0.001 \cdot S^{cap}$	(8)
S^{RBC}	135 μm$^2 \cdot N^*$	
$S^{t\ cell}$	$3 \cdot S^{cap}$	
PS^{salt}	2,500 ml/min	(31)
PS^{alb}	6 ml/min	(3)
PS^{glob}	0 ml/min	
PS^{dex}	2 ml/min	(3)

σ, reflection coefficient; L_p, hydraulic conductivity; S, surface area; PS, permeability-surface area product. Definitions of superscripts are the following: alb, albumin; glob, globulin; dex, dextran; EC, endothelial cell; br, brain capillary; cap, capillary; RBC, red blood cell; and t cell, tissue cell. * $N = (\text{Hct} \cdot \text{BV}) \cdot (94\ \mu\text{m}^3 \cdot \text{cell}^{-1})^{-1}$, where Hct is hematocrit, and BV is blood volume in μm^3. Nos. in parentheses are references. See text for more information.

the pore and the endothelium (σ^{pore} and σ^{EC}, respectively) according to the expression (7)

$$\sigma^{cap} = \beta^{EC}\sigma^{EC} + \beta^{pore}\sigma^{pore} \quad (3)$$

where β is the fraction of volume flow and $\beta^{EC} = \alpha^{EC}L_p^{EC\ br}/L_p^{cap}$ and $\beta^{pore} = \alpha^{pore}L_p^{pore}L_p^{cap}$. Although not used explicitly in the model, the value of σ^{cap} for salt calculated with the appropriate membrane properties in Table 2 is 0.14. This value agrees well with measured values of σ^{cap} for sodium chloride (22). The reflection coefficients for albumin and dextran in the pore are approximately those calculated for the entire capillary wall, and the experimentally determined PS products represent diffusional solute transport through the pores. Haraldsson et al. (5) report that σ for Dextran 70 increases with decreasing dextran concentration. The value of $\sigma = 0.8$ employed for the model is based on their results for a small total dextran concentration in plasma (<2%).

The flows of water and solute across membranes are described by equations of irreversible thermodynamics (9) and are a function of the driving "forces", namely the gradients of hydrostatic and osmotic pressure and concentration. In this model, the volume flows (J_v, ml/min) are

$$\begin{aligned}
J_v^{EC\ lum} &= L_p^{EC}S^{EC}[-\Delta\pi^{salt} - \pi^{dex} - \pi^{pp}] \\
J_v^{EC\ abl} &= L_p^{EC}S^{EC}[(P^{EC} - P^{int}) - \Delta\pi^{salt} \\
&\quad + \pi^{alb} + \pi^{dex}] \\
J_v^{pore} &= L_p^{pore}S^{pore}[(P^{cap} - P^{int}) - \sigma^{alb}\Delta\pi^{alb} \\
&\quad - \sigma^{dex}\Delta\pi^{dex} - \sigma^{glob}\pi^{glob}] \\
J_v^{RBC} &= L_p^{RBC}S^{RBC}[-\Delta\pi^{salt} + \pi^{pp} + \pi^{dex}] \\
J_v^{t\ cell} &= L_p^{t\ cell}S^{t\ cell}[-\Delta\pi^{salt} - \pi^{alb} - \pi^{dex}]
\end{aligned} \quad (4)$$

and the solute flows through the pores (J_s, g/min) are

$$\begin{aligned}
J_s^{salt} &= \overline{C}^{salt}(1 - \sigma^{salt})J_v^{pore} + PS^{salt}\Delta C^{salt} \\
J_s^{alb} &= \overline{C}^{alb}(1 - \sigma^{alb})J_v^{pore} + PS^{alb}\Delta C^{alb} \\
J_s^{dex} &= \overline{C}^{dex}(1 - \sigma^{dex})J_v^{pore} + PS^{dex}\Delta C^{dex}
\end{aligned} \quad (5)$$

where S is surface area (cm^2), P is hydrostatic pressure (mmHg), π is osmotic pressure (mmHg), C is concentration (g/ml), $\overline{C}$ is mean average concentration (g/ml), and the superscripts are the following: EC, endothelial cell; lum, luminal; abl, abluminal; RBC, red blood cell; pp, plasma proteins; cap, capillary; int, interstitium; alb, albumin; dex, dextran; t cell, tissue cell; and glob, globulin. The solute flow *Eq. 5* is a linear approximation to the exact equation given by Patlak et al. (18); however, in this model the difference between the two was calculated to be <0.1% so the simpler linear form was used. The positive direction of the volume and solute flows is shown in Fig. 1.

The initial values ($t = 0$) of the pressures and concentrations input to the flow equations are given in Table 3. These values for the compartments represent the normal state before fluid infusion. Most of these values are affected during fluid infusion and the mathematical description of these changes gives a set of auxiliary equations. In addition to fluid shifts into the plasma volume that occur across membranes, fluid is also returned to the plasma by the lymphatic system and eliminated by the kidneys. These modes of fluid exchange and interstitial compliance have also been included.

TABLE 3. *Initial values for pressures and concentrations*

Compartment	P	C^{salt}	π^{salt}	C^{alb}	π^{alb}
Plasma	20.8	0.902	5656.2	4.5	17.3
Red blood cell	20.8	0.906	5681.8		
Endothelium	20.8	0.906	5681.9		
Interstitium	0	0.902	5657.6	2.0	3.5
Tissue cell	0	0.903	5661.1		

	C^{glob}	π^{glob}	C^{dex}	π^{dex}
Plasma	2.5	8.3	0	0
Red blood cell				
Endothelium				
Interstitium			0	0
Tissue cell				

Pressure values (P, π) are measured in mmHg; Concentration values are measured in g/100 ml. Definitions for superscripts are the following: alb, albumin; glob, globulin; and dex, dextran. See text for further information.

The cell membrane does not support a difference in hydrostatic pressure, so intracellular and neighboring extracellular hydrostatic pressures are equal and fluid is driven only by an osmotic gradient. An exception is the abluminal endothelial membrane of the capillary wall, that supports a hydrostatic pressure difference between the interstitium and the plasma. The translocation of interstitial fluid during hemorrhage, transcapillary refill, results in part from a reduced capillary hydrostatic pressure. As there is no relationship to predict capillary hydrostatic pressure with changes in blood volume, it is assumed to remain constant after hemorrhage, and the model is compared with experimental results after the hemorrhage period.

The compliance of the interstitium, the change in interstitial volume for a unit change in interstitial pressure, limits how much water the interstitium can take in or give up. A three-phase linear relationship can be constructed from the data of Eliassen et al. (1) for an interstitial pressure of 0 mmHg under resting conditions. The expression for compliance is

$$\begin{aligned} \Delta V^{int} &= 1.7\ \Delta P^{int}; & P^{int} &< 0\ \text{mmHg} \\ \Delta V^{int} &= 1.2\ \Delta P^{int}; & 0 \le P^{int} &< 4\ \text{mmHg} \\ \Delta V^{int} &= 0.5\ \Delta P^{int}; & P^{int} &\ge 4\ \text{mmHg} \end{aligned} \quad (6)$$

where ΔP^{int} and ΔV^{int} are change in interstitial pressure (mmHg) and volume (liter), respectively.

Imbalances in electrolyte (salt) concentration normally do not exist in the body, since they are quickly rectified by water movement. The introduction of a hyperosmotic solution into the blood, however, creates a nonphysiological state with a severely altered plasma osmolarity that generates an enormous osmotic pressure gradient. A 7.5% NaCl solution (2,400 mosmol/l) mixes in part with the blood but each 1-mosmol/l change in osmolarity gives rise to an additional pressure of 19 mmHg.

The oncotic pressure in the plasma, i.e., the osmotic pressure exerted by the impermeable protein molecules, is a nonlinear function of total protein concentration given by the empirical formulation (11)

$$\pi^{pp} = 2.1 \cdot C^{pp} + 0.16 \cdot C^{pp\,2} + 0.009 \cdot C^{pp\,3} \quad (7)$$

where C^{pp} is the combined protein concentrations (g/100 ml) of albumin, globulins, and other impermeant molecules. Because albumin does leak slowly across the capillary membrane, it is also necessary to use the empirical osmotic pressure-concentration relation (11)

$$\pi^{alb} = 2.8 \cdot C^{alb} + 0.18 \cdot C^{alb\,2} + 0.012 \cdot C^{alb\,3} \quad (8)$$

where C^{alb} is albumin concentration (g/100 ml). The oncotic pressure of the globulins (including other impermeants) is the difference of *Eqs. 7* and *8*. Interstitial changes in osmotic pressure are taken to be linearly dependent on albumin concentration (van't Hoff relation) with 1 g/100 ml = 1.75 mmHg, since the concentration is normally a small value.

Dextran 70 emulates the oncotic property of albumin and is iso-oncotic at a concentration of ~4 g/100 ml. A 6% Dextran 70 solution (6 g/100 ml) has an osmotic pressure of 70 mmHg, and the changes in osmotic pressure with concentration can be determined from a cubic fit to experimental data (28)

$$\pi^{dex} = 6.12 \cdot C^{dex} + 0.93 \cdot C^{dex\,2} - 0.005 \cdot C^{dex\,3} \quad (9)$$

where C^{dex} is dextran concentration (g/100 ml). The osmotic pressure of dextran in the interstitium is taken to be linearly related to interstitial concentration with 1 g/100 ml = 5 mmHg.

The lymphatic system is treated as a single flow passage that transports fluid and solute from interstitium to plasma with the flow dependent only on the hydrostatic pressure in the interstitium. It is assumed that lymph has the same composition as interstitial fluid. Equations for lymphatic flow (L) were adapted from the analysis of Pirkle and Gann (20) for a resting interstitial pressure of 0 mmHg. The resulting expression is

$$\begin{aligned} L &= 1.4\ \text{ml/min}; & P^{int} &< 0\ \text{mmHg} \\ L &= 7.35 \cdot P^{int} + 1.4\ \text{ml/min}; & 0 \le P^{int} &< 4\ \text{mmHg} \\ L &= 30.8\ \text{ml/min}; & P^{int} &\ge 4\ \text{mmHg} \end{aligned} \quad (10)$$

The initial hydrostatic and osmotic pressures in Table 3 were adjusted so that a slight excess filtration into the interstitium was balanced by the lymphatic fluid return to the plasma.

Fluid is normally excreted by the kidneys at a rate of ~1 ml/min. After blood loss, renal vasoconstriction reduces the amount of blood filtered, and for a 20% hemorrhage urine output is taken to decrease to 35% of normal. A linear excretion (E)- blood volume (BV) relationship is assumed between endpoints and the expression is

$$\begin{aligned} E &= 1\ \text{ml/min}; & BV &\ge 5\ \text{L} \\ E &= 0.65 \cdot BV - 2.25\ \text{ml/min}; & 4\ \text{L} \le BV &< 5\ \text{L} \\ E &= 0.35\ \text{ml/min}; & BV &< 4\ \text{L} \end{aligned} \quad (11)$$

with BV in liters. The elimination of solutes is not considered in this simplified excretion term, and the observed diuresis incurred with hypertonic solutions (10, 17, 27) is not modeled.

Equations 3–11 comprise the mathematical basis of the model for the determination of compartmental volume changes. A computer program was written to solve for the flows numerically using the initial conditions given in Tables 1–3. The model is perturbed at $t = 0$ with an instantaneous hemorrhage and the start of fluid infusion of known composition. The blood loss depletes both plasma (water + solutes) and red blood cells. The new electrolyte, protein, and dextran (if present in the replacement fluid) concentrations are computed for the plasma compartment using the volume of infused fluid added to the current plasma volume. The J_v and J_s equations are then solved, and the new volumes and solute concentrations (osmotic pressures) are determined for all compartments. Interstitial compliance, lymphatic fluid return, and excretion are also computed and their effects incorporated into the appropriate compartments. This iterative process continues for each time step during and after the infusion period.

Equations 4 and *5* are first-order linear differential equations that can be approximated as a change in volume (dV) and solute mass (dm), respectively, divided by a time interval (dt). The approximation approaches the instantaneous derivative as the time interval, chosen as 0.1 s, tends toward zero. The quantity of material transported across the membrane is then the flow times the time interval (converted to minutes for compatible units). For example, the PV at a time after infusion $t + \Delta t$ is

$$\mathrm{PV}(t + \Delta t) = \mathrm{PV}(t) + [J_v^{\mathrm{EC\,lum}} + J_v^{\mathrm{pore}} + J_v^{\mathrm{RBC}} + \mathrm{L} - \mathrm{E}]\Delta t \quad (12)$$

Corresponding equations are written for each fluid compartment and for solute mass in the plasma and interstitial compartments.

Animal experiments. The experiments were performed on 13 male New Zealand White rabbits weighing between 0.8 and 0.9 kg. The animals were first given 1 ml of diazepam (5 mg/ml im) as a relaxant. After 10 min, they were anesthetized with 20% urethan (5 mg/kg body wt) injected intravenously into the ear which had been numbed with xylocaine. They were placed in a supine position on a heating pad that was thermostatically controlled to maintain a rectal temperature of 37°C. The animals were intubated but allowed to breathe freely throughout the experiment. The right carotid artery and jugular vein were isolated and cannulated with catheters of polyethylene tubing (PE–50). The arterial catheter was used to monitor blood pressure and to extract blood. The venous catheter allowed booster doses of anesthesia (1–2 mg) to be given as needed and infusion of the hyperosmotic solution. Before the start of each experiment, in the 30 min that the animal was allowed to stabilize, the arterial pressure was verified to be in the normal range.

The animals were bled of 15 ml (~20% of their blood volume) from the arterial catheter within 1 min. Three minutes posthemorrhage, a 7.5% NaCl-6% Dextran 70 solution was administered through the venous catheter as rapidly as possible (~10 s) to simulate a bolus dose. The infusion volume was equal to one-seventh of the shed blood volume, a value that was predicted by the mathematical model a priori to reestablish blood volume. Blood samples were taken from the arterial catheter in heparinized microhematocrit tubes before and after bleeding, every 5 s in the first minute and then at 5, 10, 30, and 60 min after the start of reinfusion. In six experiments, blood was collected in heparinized containers at these time intervals for hemoglobin determination.

The microhematocrit tubes were sealed and spun in an IEC MB centrifuge (Damon, Needham Heights, MA) at 11,500 rpm for 5 min and the hematocrits measured with a microhematocrit capillary tube reader. In five experiments, the tubes were broken and the plasma collected for the determination of plasma osmolality. The osmolality (mmol/kg H_2O) was measured with a vapor pressure osmometer (5100C, Wescor, Logan, UT) in triplicate for each sample and the values averaged. In six experiments, 20 μl of blood was mixed with 5.0 ml of a lysing reagent (Sigma, St. Louis, MO) and the hemoglobin content measured with an absorbance technique (540 nm) using a spectrophotometer (DU-40, Beckman, Fullerton, CA).

Statistical analysis. Results from the experiments are expressed as the mean of percent changes ± 1 SD. A Student's paired t test was used to determine whether hemorrhage or hyperosmotic infusion caused a significant change in hematocrit, hemoglobin concentration, or plasma osmolality. A value of $P < 0.05$ was considered statistically significant.

RESULTS

The experimental results for the changes in systemic hematocrit, hemoglobin concentration, and plasma osmolality are presented with the corresponding values calculated from the mathematical model. This comparison is made to verify the model prediction of plasma volume that is directly related to these parameters. Because the changes in plasma volume are interdependent with fluid flows from all other compartments, the validation of the model with respect to plasma volume suggests that the model is successful in describing osmotic activity throughout the body after hyperosmotic infusion.

Figure 2 shows the experimental points for systemic hematocrit at control, immediately posthemorrhage, and at intervals in the first minute and first hour after the start of hyperosmotic infusion. The mean hematocrit in 13 experiments decreased 15% from 41.0 ± 2.2 to 35.0 ± 3.4 after hemorrhage presumably due to fluid influx as a result of a reduction in capillary pressure. At the start of reinfusion, model and experiment are compared directly with the input value for hematocrit to the model equal to the experimental value at $t = 0$. The model is not modified to account for the observed transcapillary filling, since the decrease in interstitial volume is small (<5%). Model and experiment show a rapid reduction in hematocrit during the 10-s infusion period with a reversal to a stable but reduced steady-state value over the next hour ($P < 0.005$).

Changes in hemoglobin concentration from six experiments are shown in Fig. 3 together with model computations. The percent drop in hemoglobin after hemorrhage (experimental results with a control value of 12.5 g/dl blood) is very similar to that for hematocrit. With reinfusion, however, there is the continual rapid reduction in hemoglobin as was seen with hematocrit but of lesser magnitude and with no reversal immediately after the stop of infusion. Hemoglobin values remain reduced during the hour observation period ($P < 0.025$).

The comparison between experiment and model for plasma osmolality is shown in Fig. 4. The mean experimental values from five experiments are not significantly different in the control and posthemorrhage periods. During the infusion period, however, there is a sharp rise in osmolality to 64% above control, from 280 to 460 mmol/kg. This is much higher than the 15.4% predicted by the model indicating a lack of complete mixing in the initial portion of the experiment. In the hour after infusion, the plasma osmolality remains elevated by 5%

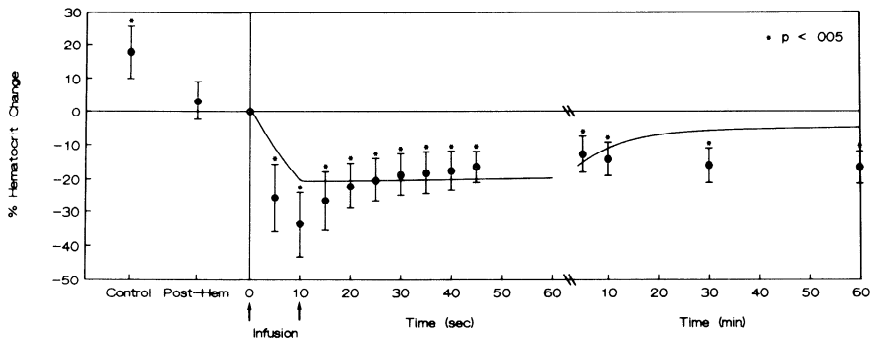

FIG. 2. Systemic hematocrit changes at time intervals throughout defined experimental procedure. Experimental points are means ± SD from 13 experiments. Sharp initial drop in hematocrit with hyperosmotic infusion is due to an osmotic fluid shift into plasma from extravascular fluid compartments and the shrinkage of red blood cells. Model (——) accounts for both effects and describes accurately trend and magnitude in hematocrit.

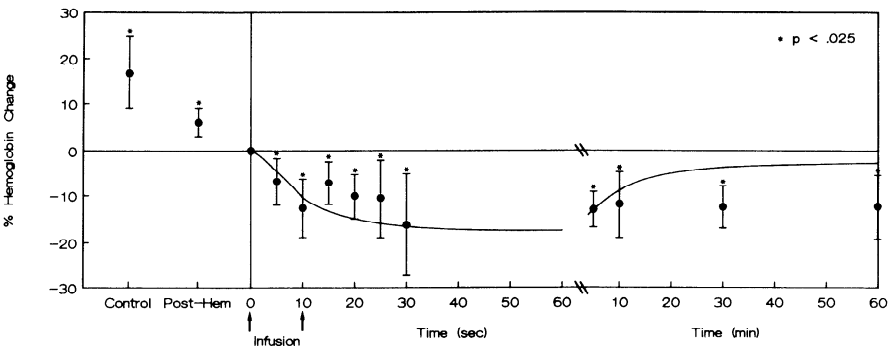

FIG. 3. Hemoglobin concentration changes from 6 experiments expressed as means ± SD. Model (——) agrees with experimental results in showing that there is a steady dilution of hemoglobin in first minute after start of hyperosmotic infusion. This effect is sustained over the next hour, and like hematocrit is underestimated by the model at these later times, indicating that other mechanisms in addition to an osmotic mechanism may be acting to retain plasma volume.

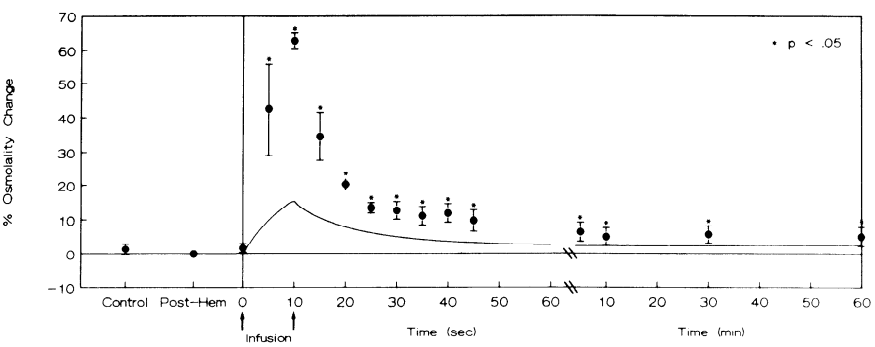

FIG. 4. Plasma osmolality changes from 5 experiments expressed as means ± SD. There is a rapid peak in osmolality occurring immediately after infusion that greatly exceeds result of model (——), which is based on a lumped plasma compartment. This transient effect indicates incomplete mixing, and experimental plasma osmolality is probably more representative of whole body several seconds after infusion.

($P < 0.05$), slightly more than predicted by the model.

The primary osmotic effects are seen to take place in the first minute after the start of the infusion. Figure 5*A* shows for this time interval the model percent volume increases for the plasma and blood volumes. The plasma volume rises to 7% above control, and the blood volume comes to within 3% of control as fluid is redistributed from the intracellular compartments and the interstitium. The volume changes for each of the intracellular compartments is shown in Fig. 5*B*. The red blood cells and endothelium that are contiguous with the plasma compartment initially lose volume but partially regain this fluid as the plasma becomes diluted. The tissue cells, however, are not in direct contact with the plasma and steadily give up water as the interstitial salt concentration rises.

Fluid shifts continue to take place between intra- and extracellular compartments and across the capillary wall until the salt concentration throughout the extracellular space is the same. Model calculations show that salt equilibration occurs within the extracellular space ~30 min after infusion. At this time, all intracellular compartments are reduced in fluid volume by 2.9%, and this fluid now resides in the plasma (volume increase of 5.6% from posthemorrhage) and the interstitium (volume increase of 5.9%).

DISCUSSION

The osmotic effects of hyperosmotic fluid infusion into the blood after hemorrhage have been described with a mathematical model that merges basic physical principles and physiological information and is supported by experimental results. It is shown that for the case of a 20% hemorrhage with 10-s reinfusion of a 7.5% NaCl-6% Dextran 70 solution equal to one-seventh of the shed blood volume, plasma volume temporarily increases over control values, and blood volume is reestablished in the first minute. The indicators of fluid influx into the plasma that were used in this study, systemic hematocrit and hemoglobin concentration, agree well with the model in the first 30 min after reinfusion. After this time, the model underestimates plasma volume suggesting that in addition to the osmotic mechanism of plasma expansion, other volume compensatory mechanisms may be operative.

The expansion in plasma volume is transitory, and this is the most likely explanation why other studies report moderate (17), or in one case, no expansion (29)

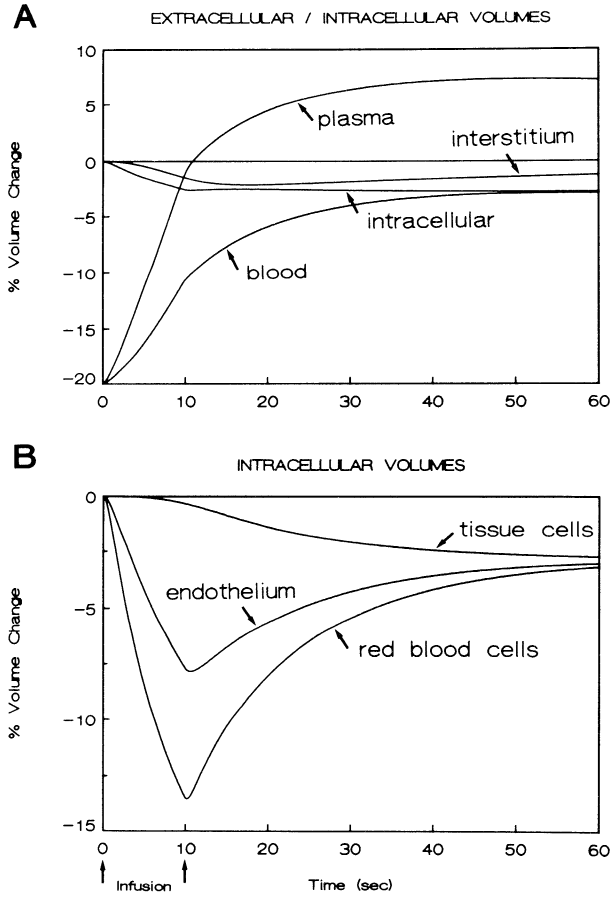

FIG. 5. Model calculations for compartmental volumes in the first minute after start of infusion under specified resuscitative conditions. *A*: volume changes in extracellular compartments (plasma and interstitium), combined intracellular compartments, and blood (plasma plus red blood cells). Restoration of blood volume to within 3% of control at end of the minute is result of fluid influx from interstitium and intracellular compartments. *B*: cellular fluid is withdrawn first from red blood and endothelial cells and then the tissue cells.

with hypertonic saline or hypertonic saline-dextran solutions, since in their studies the first measurement of plasma volume was taken several minutes after infusion. Smith et al. (27) using 7.5% NaCl-6% Dextran 70 after a 2-h period of severe blood loss show that 10 min after infusion, plasma volume is virtually restored to its baseline value and is maintained for the next hour. These findings agree with the trend in our results, however, they cannot be compared in terms of the initial plasma volume expansion, since measurements were not made immediately after infusion.

The most important finding of this investigation is the initial rapid fluid influx, within seconds, into the vasculature. This effect is due to the sudden hypertonic state of the plasma, induced by both the high salt concentration and the short infusion time. Fluid is shifted out of intracellular spaces into the extracellular compartment, and this causes dilution of the plasma constituents until osmotic balance is achieved. During this process the added salt continuously moves down its concentration gradient into the interstitium. Water accompanies the salt to maintain the osmotic balance, and since only a small amount of salt is actually added to the plasma in hypertonic resuscitation, not much fluid is retained once the salt has equilibrated.

Preventing this water leakage is the motivation for adding Dextran 70 to the solution. Its oncotic pressure offsets part of the salt transit across the capillary and thus partitions a larger proportion of the intracellular fluid into the plasma. The model predicts that with the rapid infusion of the one-seventh dose of 7.5% NaCl-6% Dextran 70 solution after a 20% hemorrhage, blood volume expands to 83.0% of its control value after 30 min compared with 80.4% when no dextran is added to the hypertonic saline (by comparison, 100% will equal complete blood volume restoration). Thus the addition of Dextran 70 increases blood volume by 2.6% or 130 ml in a 70-kg person. A 24% dextran concentration added to the hypertonic saline infusion volume would increase expansion to 92.0%. The increased viscosity of the solution, however, could limit the rate of fluid delivery.

Smith et al. (27) experimentally compared 7.5% NaCl and 7.5% NaCl-6% Dextran 70 in terms of blood volume expansion. They found a 13.8% augmentation in blood volume (our calculation) with hypertonic saline-dextran compared with hypertonic saline 3 h after a bolus infusion equal in volume to 10% of the 65% shed blood volume. The significant improvement in blood volume retention observed with dextran may be explained in part by the greater blood loss in their study. This favors increased fluid retention by Dextran 70, since it is confined to a smaller volume. Experiments done in sheep by these authors also show that the hypertonic saline-dextran solution produces the best resuscitation of the hypertonic solutions tested as evidenced by the sustained reestablishment of plasma volume, mean arterial pressure, and cardiac output.

Intracellular fluid loss, in addition to providing water for the plasma, may also have beneficial microcirculatory effects. The extraction of fluid from the endothelium increases the inner diameter of a capillary if we assume a fixed outer diameter. With a concomitant reduction in viscosity due to hemodilution, the hydraulic resistance in the capillary will be lowered. For capillaries with swollen endothelium, a condition that is observed after a sustained period of ischemia (4), the hydraulic resistance would be further reduced.

Figure 6 illustrates the changes in hydraulic resistance for a single capillary under the same conditions as in Figs. 2–5. The resistance (R) was calculated with the equation $R = k \cdot \mu / d^4$, where k is constant, μ is viscosity, and d is luminal capillary diameter. The separate resistance effects of endothelial volume shrinkage and hemodilution are shown for the normal capillary with the microcirculatory viscosity calculated from the expression (13): $\mu = 1.41 + 0.043 \cdot \mathrm{Hct}_{micro}$ with $\mathrm{Hct}_{micro} = 0.26 \cdot \mathrm{Hct}_{sys}$, where Hct_{micro} is microvessel hematocrit, and Hct_{sys} is the systemic hematocrit from the model. In this situation, there is a maximal decrease of resistance on the order of 10% leading to a modest improvement of flow in the normal capillary. After a period of hemorrhagic shock, however, the endothelium in the capillaries may swell thereby encroaching on the capillary lumen. The same model calculation, where the diameter is reduced by swollen endothelium from 5 to 4 μm, shows

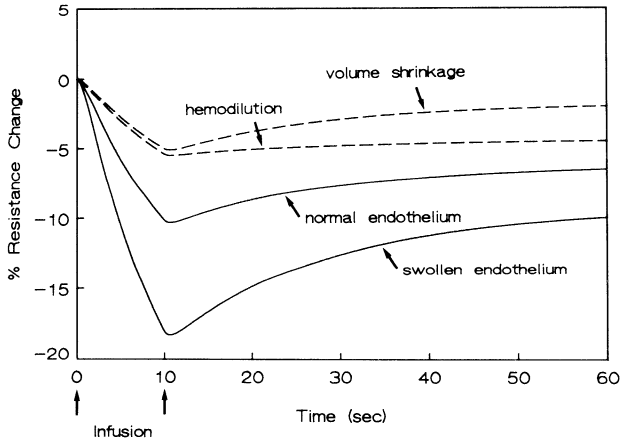

FIG. 6. Resistance changes to flow during hyperosmotic infusion in a capillary that consists of a single layer of osmotically active endothelial cells. Two situations for resistance changes are shown: one for a capillary with normal endothelium (diameter = 5 μm) and its separate effects due to hemodilution and endothelial volume shrinkage (- - - -), and second for a capillary with a lumen narrowed by swollen endothelial cells (diameter = 4 μm).

that the resistance is reduced almost 20% after hyperosmotic infusion. The more swollen the endothelium, the greater the effect of hyperosmotic solutions in reducing hydraulic resistance and improving tissue perfusion.

Evidence for cell shrinkage on exposure to hypertonic solutions has been reported for single cells, including our experimental results for red blood cells, but not for the vascular endothelium. A study by Nakayama et al. (16) with the use of membrane potential measurements demonstrates that tissue cells swell during shock and recover intracellular volume after hypertonic reinfusion. By comparison of the percent changes in hematocrit (Fig. 2) and hemoglobin concentration (Fig. 3), it is apparent that the red blood cells shrink during hyperosmotic infusion, since the magnitude of these changes differ. The changes would be identical if red blood cells, as hemoglobin, were an inert volume component in the blood, since changes in hemoglobin concentration reflect only dilution of blood components, whereas changes in hematocrit are due both to dilution and red blood cell shrinkage. Thus the difference in percent changes between hematocrit and hemoglobin concentration is an indirect measure of the decrease in red blood cell volume. In vitro experiments of red blood cell deformability with hypertonic solutions show that the cells filter easier across a porous membrane as the tonicity of the suspending medium increases (25). This is probably the direct result of the decrease in red blood cell volume. In the in vivo situation a shrunken red blood cell would have easier flow passage in the capillaries, which particularly benefits capillaries narrowed by swollen endothelium.

Fluid therapies for the treatment of blood loss have traditionally included iso-osmotic solutions such as crystalloids or colloids. For each unit of blood loss, it takes ~3 U of crystalloids or 1 U of colloids in saline to achieve adequate clinical resuscitation. The same response is obtained experimentally with very small volumes of hyperosmotic solutions. The important difference in terms of survival between the three fluid therapies is in the time it takes to reestablish stable hemodynamic conditions. Figure 7 illustrates the time it takes to expand blood volume at a reinfusion rate of 100 ml/min according to our model. In this simulation with an instantaneous 20% hemorrhage and initial 40% hematocrit, the colloid solution restores blood volume in one-half of the time of the crystalloid solution; the hyperosmotic solution (in a dose equal to one-fifth of the shed blood volume) in one-tenth of the time. At lower infusion rates, the discrepancy in times between hyperosmotic and iso-osmotic solutions is even greater.

The expansion of blood volume after hemorrhage along with vasoconstriction is essential to restoring mean arterial pressure, and the sooner this occurs, the quicker a stable circulatory condition is reached. Modig (15) in a randomized study reported a resuscitation time, the time from the start of infusion until a stable circulatory condition was achieved, of 110 ± 18 min (mean ± SD) for trauma patients treated with Dextran 70 together with isotonic Ringer acetate compared with 170 ± 40 min for treatment with Ringer acetate alone. The shorter resuscitation time with the colloid solution compared with the crystalloid agrees with our model prediction. Modig (15) attributed the significant reduction in the frequency of adult respiratory distress syndrome (ARDS) in the Dextran 70 group to the shortened shock period. The impact of hyperosmotic solutions in reducing the incidence of ARDS has not been investigated, but if rapid circulatory reestablishment is a factor, then one would expect fewer cases of ARDS after initial hyperosmotic resuscitation.

In emergency resuscitation situations, the time of patient transport may be a few minutes in an urban setting or closer to an hour for transport from a rural area. A computer model by Lewis (12) suggests that in the urban environment, the time spent starting an intravenous

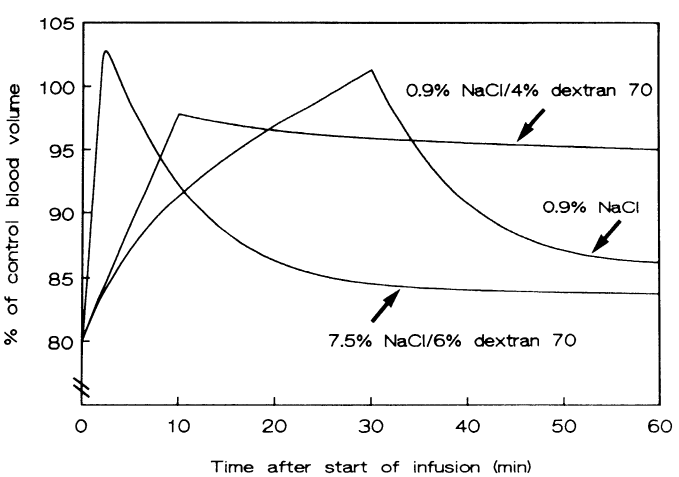

FIG. 7. Comparison of two iso-osmotic fluids, a crystalloid (0.9% NaCl) and a colloid (4% Dextran 70 in 0.9% NaCl), and a hyperosmotic fluid (7.5% NaCl-6% Dextran 70) in osmotic expansion of blood volume. It is shown that at infusion rate of 100 ml/min, a crystalloid in 3 times the volume of lost blood (20%) reestablishes blood volume after ~20 min. A dose equal to shed blood volume of a colloid achieves this state in 10 min, and a one-fifth dose of hyperosmotic solution in <2 min. Another disadvantage of crystalloid infusion is that at hour end almost 90% of infused volume has escaped from vasculature into interstitium leading in this case to a 26.7% increase in interstitial volume. This effect worsens in severe hemorrhage, where extremely large volumes of crystalloids may be infused to keep up blood volume, often resulting in pronounced tissue edema that could complicate patient recovery.

saline fluid infusion in the field may, in cases of severe hemorrhage, offset the benefit of getting the patient to the hospital sooner. But with a small volume of hyperosmotic solutions at even low infusion rates (<50 ml/min), a significant response occurs within minutes so the time spent starting an intravenous infusion in the field is justified. Also, since smaller infusion volumes are used, the risk of fluid overload in a patient incorrectly diagnosed as hypovolemic is minimized. When used as initial fluid resuscitation, a 250 ml bag of 7.5% NaCl-6% Dextran 70 rapidly injected can accommodate moderate to severe blood losses. If the initial increase in intravascular volume is not completely retained, however, on arrival to the hospital the volume can be supplemented if needed with iso-osmotic fluids and with blood or packed red blood cells for patients with a hematocrit below 30% to satisfy O_2 requirements.

Hyperosmotic solutions have been shown to be superior to iso-osmotic fluids in quickly restoring plasma volume, mean arterial pressure, and cardiac output due in part to an osmotically expanded blood volume. The efficacy of these solutions is most pronounced in emergency resuscitation situations where a trauma patient has the most to gain from an effective fluid therapy. The early rapid restoration of circulatory function after hypovolemic hemorrhage may be pivotal not only to survival but to the reduction in secondary complications manifested days after the initial trauma. To this end, hyperosmotic solutions show great promise.

We thank Michelle Biren for the excellent technical assistance.

This research was supported by National Heart, Lung, and Blood Institute Grants HL-12493, HL-17421, and HL-07089.

Address for reprint requests: M. C. Mazzoni, Dept. of Applied Mechanics and Engineering Sciences-Bioengineering R-012, Univ. of California, San Diego, La Jolla, CA 92093.

Received 21 December 1987; accepted in final form 21 April 1988.

REFERENCES

1. ELIASSEN, B., B. FOLKOW, S. M. HILTON, B. OBERG, AND B. RIPPE. Pressure-volume characteristics of the interstitial fluid space in the skeletal muscle of the cat. *Acta Physiol. Scand.* 90: 583–593, 1974.
2. FRIEDMAN, J. J. Hyperosmolality and transcapillary fluid and protein movement in skeletal muscle. *Microvasc. Res.* 29: 340–349, 1985.
3. GARLICK, D. G., AND E. M. RENKIN. Transport of large molecules from plasma to interstitial fluid and lymph in dogs. *Am. J. Physiol.* 219: 1595–1605, 1970.
4. GIDLÖF, A., F. HAMMERSEN, J. LARSSON, D. H. LEWIS, AND S.-O. LILJEDAHL. Is capillary endothelium in human skeletal muscle an ischemic shock tissue? In: *Induced Skeletal Muscle Ischemia in Man,* edited by D. H. Lewis. New York: Karger, 1982, p. 63–79.
5. HARALDSSON, B., B. J. MOXHAM, AND B. RIPPE. Capillary permeability to sulphate-substituted and neutral dextran fractions in the rat hindquarter vascular bed. *Acta Physiol. Scand.* 115: 397–404, 1982.
6. HODGKIN, A. L., AND P. HOROWICZ. The influence of potassium and chloride ions on the membrane potential of single muscle fibres. *J. Physiol. Lond.* 148: 127–160, 1959.
7. HOUSE, C. R. *Water Transport in Cells and Tissues.* Baltimore, MD: Williams & Wilkins, 1974, p. 66–76.
8. KARNOVSKY, M. J. Morphology of capillaries with special reference to muscle capillaries. In: *Capillary Permeability,* edited by C. Crone and N. A. Lassen. Copenhagen: Munksgaard, 1970, vol. 1, p. 341–350.
9. KEDEM, O., AND A. KATCHALSKY. Thermodynamic analysis of the permeability of biological membranes to non-electrolytes. *Biochim. Biophys. Acta* 27: 229–246, 1958.
10. KRAMER, G. C., P. R. PERRON, D. C. LINDSEY, H. S. HO, R. A. GUNTHER, W. A. BOYLE, AND J. W. HOLCROFT. Small-volume resuscitation with hypertonic saline dextran solution. *Surgery St. Louis* 100: 239–246, 1986.
11. LANDIS, E. M., AND J. R. PAPPENHEIMER. Exchange of substances through the capillary walls. In: *Handbook of Physiology. The Circulation.* Bethesda, MD: Am. Physiol. Soc., 1963, sect. 2, vol. II, chapt. 29, p. 961–1034.
12. LEWIS, F. R. Prehospital intravenous fluid therapy: physiologic computer modelling. *J. Trauma* 26: 804–811, 1986.
13. LIPOWSKY, H. H., S. USAMI, AND S. CHIEN. In vivo measurements of "apparent viscosity" and microvessel hematocrit in the mesentery of the cat. *Microvasc. Res.* 19: 297–319, 1980.
14. LOPES, O. U., I. T. VELASCO, P. G. GUERTZENSTEIN, M. ROCHA E SILVA, AND V. PONTIERI. Hypertonic sodium chloride restores mean circulatory filling pressure in severely hypovolemic dogs. *Hypertension Dallas* 8, *Suppl.* I: I195–I199, 1986.
15. MODIG, J. Effectiveness of dextran 70 versus Ringer's acetate in traumatic shock and adult respiratory distress syndrome. *Crit. Care Med.* 14: 454–457, 1986.
16. NAKAYAMA, S., G. C. KRAMER, R. C. CARLSEN, AND J. W. HOLCROFT. Infusion of very hypertonic saline to bled rats: membrane potentials and fluid shifts. *J. Surg. Res.* 38: 180–186, 1985.
17. NAKAYAMA, S., L. SIBLEY, R. A. GUNTHER, J. W. HOLCROFT, AND G. C. KRAMER. Small-volume resuscitation with hypertonic saline (2,400 mOsm/Liter) during hemorrhagic shock. *Circ. Shock* 13: 149–159, 1984.
18. PATLAK, C. S., D. A. GOLDSTEIN, AND J. F. HOFFMAN. The flow of solvent and solute across a two-membrane system. *J. Theor. Biol.* 5: 426–442, 1963.
19. PAULSON, O. B., M. M. HERTZ, T. G. BOLWIG, AND N. A. LASSEN. Filtration and diffusion of water across the blood-brain barrier in man. *Microvasc. Res.* 13: 113–124, 1977.
20. PIRKLE, J. C., AND D. S. GANN. Restitution of blood volume after hemorrhage: mathematical description. *Am. J. Physiol.* 228: 821–827, 1975.
21. PLYLEY, M. J., AND A. C. GROOM. Geometrical distribution of capillaries in mammalian striated muscle. *Am. J. Physiol.* 228: 1376–1383, 1975.
22. RENKIN, E. M., AND F. E. CURRY. Transport of water and solutes across capillary endothelium. In: *Membrane Transport in Biology,* edited by G. Giebisch, D. C. Tosteson, and H. H. Ussing. New York: Springer-Verlag, 1979, vol. IVA, p. 1–45.
23. ROCHA E SILVA, M., G. A. NEGRAES, A. M. SOARES, V. PONTIERI, AND L. LOPPNOW. Hypertonic resuscitation from severe hemorrhagic shock: patterns of regional circulation. *Circ. Shock* 19: 165–175, 1986.
24. SHA'AFI, R. I., G. T. RICH, V. W. SIDEL, W. BOSSERT, AND A. K. SOLOMON. The effect of the unstirred layer on human red cell water permeability. *J. Gen. Physiol.* 50: 1377–1399, 1967.
25. SLATER, N. G. P., J. VYAS, D. LOVETT, T. C. PEARSON, AND A. J. GRIMES. Filterability of red cells in iron deficiency. *Clin. Hemorheol.* 2: 373–381, 1982.
26. SMAJE, L. H., B. W. ZWEIFACH, AND M. INTAGLIETTA. Micropressure and capillary filtration coefficients in single vessels of the cremaster muscle of the rat. *Microvasc. Res.* 2: 96–110, 1970.
27. SMITH, G. J., G. C. KRAMER, P. PERRON, S. NAKAYAMA, R. A. GUNTHER, AND J. W. HOLCROFT. A comparison of several hypertonic solutions for resuscitation of bled sheep. *J. Surg. Res.* 39: 517–528, 1985.
28. THOREN, L. 1978. Dextran as a plasma volume substitute. In: *Blood Substitutes and Plasma Expanders,* edited by G. A. Jamieson and T. J. Greenwalt. New York: Liss, 1978, p. 265–282.
29. VELASCO, I. T., V. PONTIERI, M. ROCHA E SILVA, AND O. U. LOPES. Hyperosmotic NaCl and severe hemorrhagic shock. *Am. J. Physiol.* 239 (*Heart Circ. Physiol.* 8): H664–673, 1980.
30. WILDENTHAL, K., D. S. MIERZWIAK, AND J. H. MITCHELL. Acute effects of increased serum osmolality on left ventricular performance. *Am. J. Physiol.* 216: 898–904, 1969.
31. YUDILEVICH, D. L., E. M. RENKIN, O. A. ALVAREZ, AND I. BRAVO. Fractional extraction and transcapillary exchange during continuous and instantaneous tracer administration. *Circ. Res.* 23: 325–336, 1968.